

Contribution of H₂ plasma etching to radial profile of amount of dust particles in a divertor simulator

M Tateishi¹, K Koga¹, D Yamashita¹, K Kamataki², H Seo¹, N Itagaki^{1,3},
M Shiratani¹, N Ashikawa⁴, S Masuzaki⁴, K Nishimura⁴, A Sagara⁴
and the LHD Experimental Group⁴

¹ Faculty of Information Science and Electrical Engineering, Kyushu University, 744 Motooka, Nishi-ku, Fukuoka 819-0395, Japan.

² Faculty of Arts and Science, Kyushu University, 744 Motooka, Nishi-ku, Fukuoka 819-0395, Japan.

³ PRESTO Japan Science and Technology Agency, 5 Sanban-cho Chiyoda-ku Tokyo, 102-0075, Japan.

⁴ National Institute for Fusion Science, 322-6 Oroshi-cho Toki-city Gifu, 509-5292, Japan.

E-mail: m.tateishi@plasma.ed.kyushu-u.ac.jp

Abstract. We have studied contribution of H₂ plasma etching to radial profile of amount of dust particles generated due to interactions between H₂ plasmas and graphite target in a divertor simulator. Dust fluxes of spherical particles and flakes are the maximum at the distance $r = 100$ mm and 120 mm from the centre axis of the plasma column, respectively. From ion density and dust flux, we have deduced etched volume of deposited dust particles due to H₂ plasma irradiation. Sum of the etched volume and measured volume of spherical dust particles is almost constant for $r < 120$ mm and decreases with increasing r for $r > 120$ mm, whereas that of flakes is the maximum at $r = 120$ mm. H₂ plasma etching significantly reduces size of dust particles for r smaller than 100 mm.

1. Introduction

In fusion devices, dust particles generated due to plasma-wall interactions are pointed out to become safety hazard due to tritium retention and radioactive content in dust particles. Dust particles also may cause deterioration of plasma confinement [1-8]. Dust particles can easily react with oxygen and water when the reactor is exposed to air during maintenance, leading to an explosion hazard [9]. Hydrogen isotopes such as tritium trapped in them and on their surface can also react with air. Their vaporization in the edge of fusion plasmas can be a source of impurity, leading to deterioration of plasma confinement [10]. Therefore, their maximum quantity in International Thermonuclear Experimental Reactor is restricted below 6 kg of carbon or 11 kg of beryllium and 230 kg tungsten [11, 12]. To overcome these issues, it is important to understand their generation and transport mechanisms in fusion devices. So far, we have developed a divertor simulator using helicon discharges to study generation and transport mechanisms of dust particles. Using the discharges, we have simulated generation of dust particles in nanometer size due to interaction between plasmas and graphite target, which is employed as a divertor material in Large Helical Device (LHD) [13-17]. For the dust collection experiments, collected dust particles are exposed by irradiation of H₂ plasma, leading to



etching of dust particles. The contribution of the H_2 plasma etching may be important to evaluate the amount of collected dust particles. Here we estimated such contribution to radial profile of amount of dust particles. The results give insight on the etching effect on dust particles re-deposited in nuclear fusion devices.

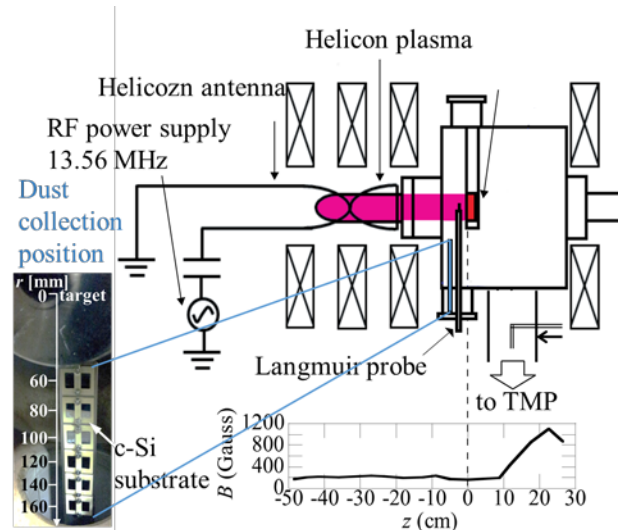


Figure 1. Experimental set up of the divertor simulator, c-Si substrates and spatial profile of magnetic flux density on center axis of the reactor. c-Si substrates are set on a Ti holder placed at 25 mm from the target and 60, 80, 100, 120, 140 and 160 mm from the center of plasma column. The surface of substrates faces the graphite target. The inset shows the magnetic flux density in center axis of the discharge tube. The graphite target was set at $z = 0$ mm.

2. Experimental

Experiments were carried out with the divertor simulator as shown in figure 1. The reactor is composed of a stainless vessel with 267 mm maximum inner diameter and 294 mm length, a quartz tube of 50 mm diameter and 200 mm length, as well as an antenna for the $m = 1$ helicon mode excitation of 170 mm length placed around the tube [18]. The uniform magnetic field of 0.015 T (150 Gauss) was applied along the center axis of the discharge tube with the four magnetic coils. Gas of pure H_2 was supplied at 13 sccm in flow rate at pumping port to reduce effects of gas flow on dust transport. The gas pressure was 5 mTorr. H_2 plasmas were generated by applying pulsed RF voltage of 13.56 MHz to a helicon antenna. The ion density and electron temperature at the center of the discharge and 20 mm from the target was $2.8 \times 10^{12} \text{ cm}^{-3}$ and 6 eV, respectively. The ion density and electron temperature are close to those of divertor plasmas in LHD [19]. The discharging period was 0.25 s and the interval was 1.0 s to avoid over heating the quartz discharge tube. In order to produce dust particles due to interactions between the carbon wall and the H_2 plasmas, a polycrystalline graphite target (Toyo Tanso IG-430U) of 35 mm in diameter and 8 mm in thickness was placed as shown in figure 1. The graphite target is employed for divertor material in LHD.

Dust particles were collected on c-Si substrates set on a Ti holder placed at 25 mm from the target and 60, 80, 100, 120, 140 and 160 mm from the center of plasma column. The surface of substrates faces the graphite target. The size and shape of the dust particles collected on the substrates were measured with a scanning electron microscope (SEM). The minimum detectable particle size in the SEM measurements was 50 nm. Their composition was obtained by energy dispersive X-ray (EDX) analysis.

3. Results and Discussion

Collected dust particles can be classified into two kinds: spherical particles and flakes. EDX analysis shows that the major compositions of the dust particles are C and Fe; C is the predominant composition of the graphite target and Fe is one of compositions of the chamber materials. Carbon is the primary composition of spherical particles and flakes. The shape of spherical particles indicates they are formed in gas phase due to deposition of carbon radicals on their surface. Flakes have an irregular shape which suggest they are formed due to peeling from the carbon films deposited on the reactor wall and/or the target [4].

Figure 2 shows size distribution of dust flux as a parameter of distance r from the center of the plasma column. The flux of collected dust particles towards the substrates was obtained by

$$\Gamma_d = \frac{n(d)}{t_{\text{total}}}, \quad (1)$$

where $n(d)$ and t_{total} are the area density of dust particles with a size d deposited on a substrate and the total discharging period (581 s), respectively. All the spherical particles are smaller than 300 nm and the flakes are in a size range from 40 nm to a few μm . The peak in the size distribution is independent of r and around 50 nm for both of the spherical particles and flakes. The size distributions shows similar shape for any r . It suggests that the radial transport of the dust particles depend little on their size. Therefore, the volume of spherical particles and flakes obtained by integrating their volume between 50 nm and 1 μm in size, respectively, are employed to discuss qualitatively radial transport of dust particles.

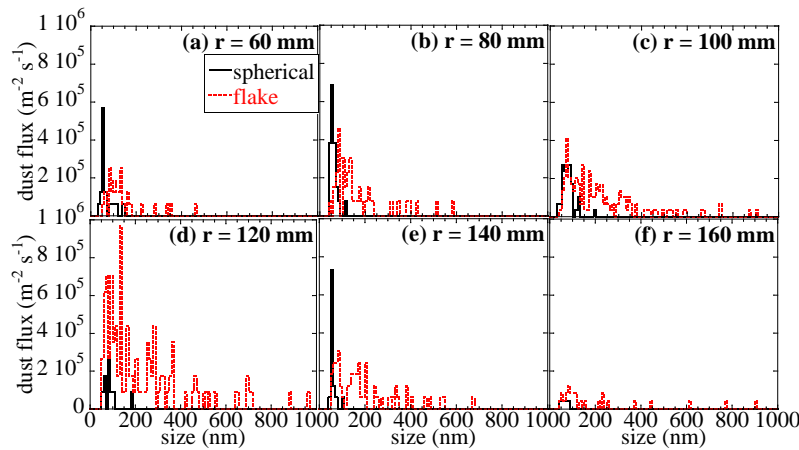


Figure 2. Size distribution of flux of collected dust particles for $r =$ (a) 60 mm, (b) 80 mm, (c) 100 mm, (d) 120 mm, (e) 140 mm, and (f) 160 mm.

Volume of collected dust particles V_{col} is given by

$$V_{\text{col}} = \int \frac{4}{3} \pi \left(\frac{d}{2}\right)^3 n(d) dd \quad \text{for spherical particles,} \quad (2)$$

$$V_{\text{col}} = \int 100 \times 10^{-9} \frac{(d)^2}{2} n(d) dd \quad \text{for flakes,} \quad (3)$$

where the volume is integrated in a size range between 50 nm and 1 μm . Thickness of flakes is assumed to be 100 nm.

During the dust collection, H_2 plasmas are irradiated to dust particles deposited on the substrates. To estimate the etching effects on the dust particles, we have evaluated from the erosion yield Y_{tot} of carbon films [20]. In this study, Y_{tot} has been employed as etching yield of the dust particles. Y_{tot} is a function

of ion energy E_0 , ion flux Γ_i and electron temperature T_e . E_0 is assumed to be the same as the difference

between substrate potential and space potential of hydrogen plasmas, because of low pressure. Γ_i is obtained from the ion density n_i and electron temperature T_e measured near the substrate. Figure 3 shows r dependence of n_i and T_e . n_i exponentially decreases with increasing r . T_e is almost constant of about 4 eV between $r = 60$ mm and 110 mm. Etched thickness of dust particles t_{etch} is given by

$$t_{etch} = \frac{\Gamma_i Y_{tot} m_c}{\rho_d} t_{total}, \quad (4)$$

As shown in figure 4, etched thickness of dust particles t_{etch} decreases from 39.2 nm for $r=60$ mm to 0.01 nm for $r=160$ mm. H_2 plasma etching reduces size of dust particles and hence some dust particles became smaller than the lower detection limit of size.

The etched volume V_{etch} of observed dust particles is given by

$$V_{etch} = \int \frac{\Gamma_i Y_{tot} m_c}{\rho_d} S t_{total} n(d) dd, \quad (5)$$

where the volume is integrated in a size range between 50 nm and 1 μ m. m_c is mass of a carbon atom. ρ_d is the mass density of the dust which is assumed to be 1.8 g/cm³ [21], the mass density of the graphite target. d is the size of a dust particle. S is given by

$$S = \pi \left(\frac{d}{2}\right)^2 \quad \text{for spherical particles}, \quad (6)$$

$$S = \frac{(d)^2}{2} \quad \text{for flakes}, \quad (7)$$

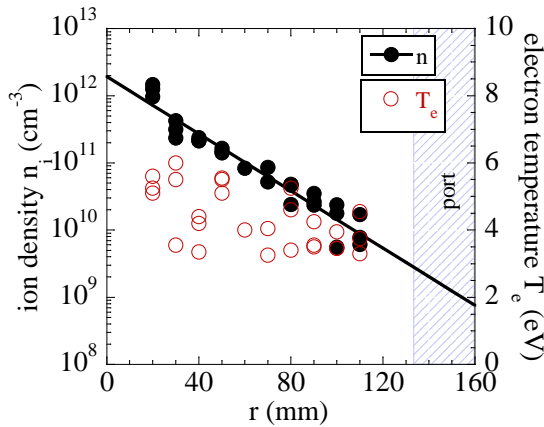


Figure 3. Distance dependence of ion density and electron temperature.

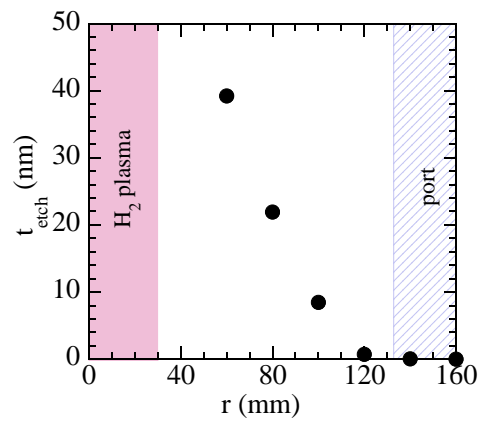


Figure 4. Distance dependence of etched thickness of dust particles.

In the eq. (4), all dust particles are assumed to be etched by H_2 plasmas during discharge period t_{total} , namely, the maximum etched volume of dust particles. Here, we neglect the growth of dust particles collected on substrates due to deposition of radicals or self-organization. We have to investigate the growth of dust particles on vessel wall in future research. Figure 5 shows r dependence of V_{col} and $V_{col} + V_{etch}$ of spherical particles is almost constant for r below 120 mm and decreases with increasing r for r above 120 mm. That of flakes has a maximum value for $r=120$ mm, suggesting that flakes are formed by peeling of re-deposited carbon films on vessel wall ($r=133.5$ mm).

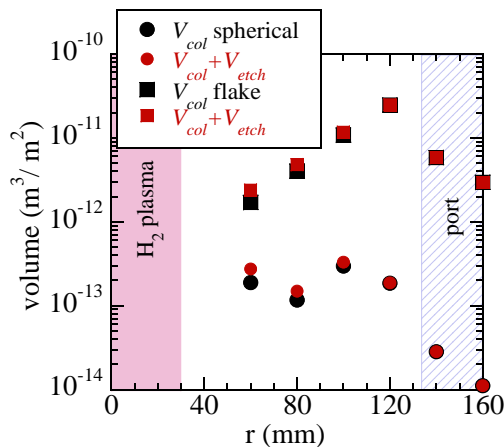


Figure 5. Distance dependence of V_{col} and $V_{col} + V_{etch}$.

Figures 6 (a) and (b) show a ration R of V_{etch} to $V_{\text{col}} + V_{\text{etch}}$ versus r and ion density at 5 mm from each collection substrate, respectively. R of spherical dust particles and flakes monotonically increasing with decreasing r and increasing n_i from 0.01 and 0.00 for $r = 160$ mm to 31.0 and 28.2 % for $r = 60$ mm, respectively. R is smaller than 1 % for r larger than 120 mm that means n_i smaller than $5.39 \times 10^9 \text{ cm}^{-3}$. Therefore, etching effects on dust particles are negligible for r larger than 120 mm. R is larger than 7 % for r smaller than 100 mm that corresponds to n_i larger than $1.47 \times 10^{10} \text{ cm}^{-3}$. These results suggest that volume of dust particles deposited on vessel wall can be reduced by H_2 plasma irradiation.

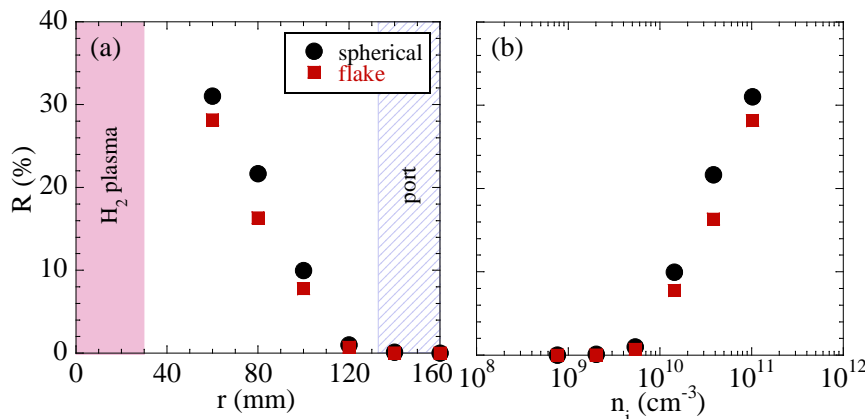


Figure 6. (a) a ration R of V_{etch} to $V_{\text{col}} + V_{\text{etch}}$ versus distance r . (b) a ration R of V_{etch} to $V_{\text{col}} + V_{\text{etch}}$ versus ion density n_i .

4. Conclusions

We have studied spatial profile of flux of dust particles generated due to interaction between H_2 plasmas and graphite target and evaluated etching of the collected dust particles due to H_2 plasma irradiation. We have obtained the following two conclusions:

1. Etching effects on dust particles are negligible for r larger than 120 mm. H_2 plasma etching significantly reduces size of dust particles for r smaller than 100 mm.
2. $V_{\text{col}} + V_{\text{etch}}$ of flakes has a maximum value for $r = 120$ mm, suggesting that the flakes are formed by peering of re-deposited carbon films on vessel wall ($r = 133.5$ mm).
3. Volume of dust particles deposited on vessel wall are reduced by H_2 plasma irradiation.

Acknowledgments

This research was supported by MEXT KAKENHI Grant Number 21110005 and General Coordinated Research Grant from the National Institute for Fusion Science Grant Number NIFS12KLPF020 and NIFS12KLPF022.

References

- [1] Winter J 2000 *Phys. Plasmas* **7** 3862-66
- [2] Sharpe J P, Petti D A and Bartels H -W 2002 *Fusion Eng. Des.* **63-4** 153-63
- [3] Muto S, Matsui T and Tanabe T 2002 *J. Nucl. Mater.* **307-11** 1289
- [4] Koga K, Uehara R, Kitaura Y, Shiratani M, Watanabe Y and Komori A 2004 *IEEE Trans. Plasma Sci.* **32** 405-09
- [5] Federici F, Coad J P, Haasz A A, Janeschitz G, Noda N, Philipps V, Roth J, Skinner C H, Tivey R and Wu C H 2000 *J. Nucl. Mater.* **283-7** 110-9
- [6] Girard J -Ph, Garin P, Taylor N, Uzan-Elbez J, Rodriguez-Rodrigo L and Gulden W 2007 *Fusion Eng. Des.* **82** 506-10
- [7] Krashennnikov S I, Pigarov A Yu, Smirnov R D, Rosenberg M, Tanaka Y, Benson D J,

- Soboleva T K, Rognlien T D, Mendis D A, Bray B D, Rudakov D L, Yu J H, West W P, Roquemore A L, Skinner C H, Terry J L, Lipschultz B, Bader A, Granetz R S, Pitcher C S, Ohno N, Takamura S, Masuzaki S, Ashikawa N, Shiratani M, Tokitani M, Kumazawa R, Asakura N, Nakano T, Litnovsky A M, Maqueda R and the LHD Experimental Group 2008 *Plasma Phys. Control. Fusion* **50** 124054
- [8] Krasheninnikov S I, Smirnov R D and Rudakov D L 2011 *Plasma Phys. Control. Fusion* **53** 083001
- [9] Denkevitis K, 2010 *Fusion Eng. and Des.* **85** 1059
- [10] Shinomura Y, 2007 *J. Nucl. Mater.* **363-365** 467
- [11] Roth J, et al., 2009 *J. Nucl. Mater.* **390** 1
- [12] Rosanvallon S, et al., 2009 *J. Nucl. Mater.* **390** 57
- [13] Koga K, Iwashita S, Kiridoshi S, Shiratani M, Ashikawa N, Nishimura K, Sagara A, Komori A and the LHD Experimental Group 2009 *Plasma Fusion Res.* **4** 34
- [14] Iwashita S, Miyata H, Koga K, Shiratani M, Ashikawa N, Nishimura K, Sagara A and the LHD Experimental Group 2009 *J. Plasma Fusion Res. SERIES* **8** 308-1
- [15] Iwashita S, Nishiyama K, Uchida G, Seo H, Itagaki N, Koga K, Shiratani M 2013 *Fusion Eng. Des.* **88** 28-32
- [16] Koga K, Nishiyama K, Morita Y, Uchida G, Yamashita D, Kamataki K, Seo H, Itagaki N, Shiratani M, Ashikawa N, Masuzaki S, Nishimura K, Sagara A and the LHD Experimental Group 2013 *J. Nucl. Mater.* **438** 727-30
- [17] Nishiyama K, Morita Y, Uchida G, Yamashita D, Kamataki K, Seo H, Itagaki N, Koga K, Shiratani M, Ashikawa N, Masuzaki S, Nishimura K, Sagara A, the LHD Experimental Group, Bornholdt S and Kersten H 2013 *J. Nucl. Mater.* **438** 788-91
- [18] Aramaki M, Kato K, Goto M, Muto S, Morita S and Sasaki K 2004 *J. Appl. Phys.* **43** 1164-65
- [19] Masuzaki S, Kobayashi M, Akiyama T, Ohno N, Morisaki T, Shoji M, Tokitani M, Tanaka H, Peterson B J, Yoshimura S, Narihara K, Yamada I, Yasuhara R, Murakami A, Miyazawa J, Murase T, Kobuchi T, Yonezu H, Kawamura G, Murakami I, Takeiri Y, Yamada H, Komori A and LHD experiment group 2013 *J. Nucl. Mater.* **438** S133-S138
- [20] Roth J 1999 *J. Nucl. Mater.* **266-9** 51-7
- [21] Koga K, Nishiyama K, Morita Y, Yamashita D, Kamataki K, Uchida G, Seo H, Itagaki N, Shiratani M, Ashikawa N, Masuzaki S, Nishimura K, Sagara A and the LHD Experimental Group 2012 Proc. 24th IAEA Fusion Energy Conf. **266** 51